A Novel Demand Response Strategy for Sizing of Hybrid Energy System With Smart Grid Concepts

ALI M. ELTAMALY[1,2,3], **MAJED A. ALOTAIBI**[4], **ABDULRAHMAN I. ALOLAH**[4], **AND MOHAMED A. AHMED**[5,6]

[1]Sustainable Energy Technologies Center, King Saud University, Riyadh 11421, Saudi Arabia
[2]Electrical Engineering Department, Mansoura University, Mansoura 35516, Egypt
[3]K. A. CARE Energy Research and Innovation Center at Riyadh, Riyadh 11451, Saudi Arabia
[4]Department of Electrical Engineering, College of Engineering, King Saud University, Riyadh 11421, Saudi Arabia
[5]Department of Electronic Engineering, Universidad Técnica Federico Santa María, Valparaíso 2390123, Chile
[6]Department of Communications and Electronics, Higher Institute of Engineering and Technology–King Marriott, Alexandria 23713, Egypt

Corresponding author: Ali M. Eltamaly (eltamaly@ksu.edu.sa)

ABSTRACT The sizing problem of the hybrid energy system (HES) is a crucial issue especially in rural communities because any wrong results can mislead the decision makers for building the new HES. Due to the intermittent nature of the renewable energy sources (RES) such as wind and PV, there will be a need for a high storage system and/or a standby diesel engine, which increase the investment, required, and increases the cost of energy (CoE). The use of smart grid concepts like the demand response (DR) using dynamic tariff can improve the system performance, enhance the stability, reduces the size and investments of HES components, reduces the customers' bills, and increases the energy providers' profits. The DR strategy will allow the customers to share the responsibility of the HES stability with the energy providers to maintain the stability of the HES. The DR strategies should be selected to ensure the balance between the available RES and the load requirements. In this article, a novel DR strategy is introduced to model the required change in the tariff with the battery state of charge and its charging/discharging power. The novel DR strategy is used in the sizing of the HES based on techno-economic objectives using three different soft computing optimization techniques. This article introduces modeling and simulation of the smart grid integrated with hybrid energy systems to supply a standalone load for a rural site in the north of Saudi Arabia. The sizing of the HES is built based on minimizing the CoE and the loss of load probability. The novel DR strategy introduced in this article reduced the size of the HES compared to the fixed load technique by 20.66%. The results obtained from this novel strategy proved its superiority in the sizing and operation stage of the HES.

INDEX TERMS Hybrid energy system, smart grid, demand response, dynamic tariff, wind, photovoltaic, diesel, PSO.

I. INTRODUCTION

The renewable energy sources (RES) such as wind and PV became a very attractive option for generating electricity in the rural communities as well as for the central power stations. The intermittent nature of these RES will need a conventional power sources and/or storage systems to improve their reliability. For this reason, the RES should be connected with a battery system and a Diesel generator to have a stable hybrid energy system (HES). The HES can be connected with the electric utility network which is called "on-grid" and it

The associate editor coordinating the review of this manuscript and approving it for publication was Qiuye Sun.

can be work as a standalone system which is called "off-grid". The proposed study shown in this article is dealing with the off-grid HES only. The off-grid systems are used to feed rural communities away from the electric utility with their needs from electricity using RES which reduces the dependence of these communities on the fossil fuels and avoids the problem of securing enough amount of fuels in these rural sites which may be become a great challenge. Moreover, the cost of energy (CoE) from HES is much lower than the one associated with fossil fuel generators. For this reason, the off-grid HES system is counted as the best option for electricity generation in rural communities. The sizing of the HES should be performed before the installation of the

system. There are many efforts that have been introduced in the literature to perform the sizing study. The system configurations have been discussed in [1], [2] to select the best configuration, where the PV, wind, battery, Diesel, and/or hydrogen storage tanks are the most famous components in the modern HES. Many configurations have been introduced in the literature, [2]–[6], most of these configurations are using wind and PV energy system as RES [2], [3]. Some other studies introduced other sources of renewable energies [4], [5]. Most of these studies used battery and/or Diesel generators as a first backup source [2], [3], and some other studies used some other storage systems [6]. The different energy storing devices that can be used to store electrical energy are classified and discussed in [7], [8].

The optimal sizing of the HES has been carried out in many studies using different optimization techniques for different techno-economical objective functions. The most objective functions used for optimal sizing of the HES are the minimization of the cost of energy [2], [3], the loss of load probability [9], and the greenhouse gas emission.

Different strategies have been introduced in the literature to perform CoE estimation, some of these strategies used net present cost (NPC) [10]. The NPC can give an estimation of the CoE in each year and cash flow through the operation of the system [11], [10]. Another strategy uses the life cycle cost (LCC) in which the total initial cost of the HES and the all operating, replacements, and the salvage prices are calculated at the beginning of the paper and the Levelized cost of energy (LCE) can be calculated dividing the total LCC by the total energy expected from the HES through its life span [12], [3]. Another cost study called annualized cost system (ACS) has been used in [13]. One of the best cost analysis for the HES is the CoE strategy in which the ratio of the total annualized cost of the system to the yearly electricity delivered to the load [14], [15]. A detailed description of these cost estimation strategies is introduced in [16].

Different reliability indices were introduced in the literature to model the shortage of the energy in the HES system such as loss of load probability (*LOLP*) or loss of energy expected (LEE) that should be minimized to secure the energy for the customers during the year. The lower values of reliability indices the higher the size of the HES components which can be translated to an increase in CoE. Therefore, searching for a technology that can reduce these indices without increasing the HES size and CoE is a great challenge which is tackled by the use of the smart grid as will be shown in this study.

Under the highly dynamic nature of the generated power, varying consumer demand, and CoE, the smart grid should manage the system such that the load demand is met by giving a higher priority to RES. Most of the sizing studies introduced in the literature did not take the concepts of the smart grid into considerations. Some studies divided the loads into two categories, the high priority loads and low priority loads [9], [17]–[19]. The high priority loads should be covered and the low priority loads can be shifted from the

periods of shortage of generations to the high generations periods. The demand response (DR) as a one of the smart grid concepts (SGC) is used in the operation of the HES but still there are no studies shown in the literature taking the DR into considerations in the sizing stage of the HES.

The nonlinear sizing problem has been tackled using optimization techniques. The first technique to solve the sizing problem of the HES was using the graphical construction technique (GCT) [20], [21]. The GCT should be used to optimize only one variable and the other variables should be estimated. For this reason, the GCT does not give the optimal solution for the sizing problem. The iterative approach has been used also in the sizing of HES by using nested loops for each variable needs to be optimized with increment change in these variables is used in many studies [22]–[24]. This technique is taking a long time to perturb each variable and the results obtained is depending on the increment in each variable. Another sizing technique called probabilistic approach which is work based on the effects of random variability up on the performance of a system [25], [26]. This technique is easy to implement but it cannot produce accurate results with the dynamic change of the HES. Another method called trade-off method is working based on compromising between the different variables to get an acceptable solution [27]. The soft computing techniques have been widely used in solving the sizing problems using many optimization techniques like particle swarm optimization (PSO) [15], Cuckoo Search (CS) [9], genetic algorism (GA) [2], firefly optimization (FFO) [28], gray wolf optimization (GWO) [29], harmony search (HS) [30], simulated annealing (SA) [31], artificial bee colony (ABC) algorithm [32], crow search algorithm (CSA) [33], etc. These optimization techniques are characterized by fast and accurate results, but, in some cases, it may be trapped in premature convergence in case of inaccurate value of their control parameters are chosen. These disadvantages can be overcome using a suitable tuning study or a comparison with other similar optimization techniques as will be introduced in this article.

In this article, a proposed model of a smart grid integrated with HES is developed. As many HES configurations, the proposed system in this article is containing wind energy systems (WES), PV energy system (PVES), batteries, Diesel Engine (DE), loads, and the power electronics converters (PEC). A real load for a rural city in the north of Saudi Arabia has been selected to be used in the design stage of the proposed HES. The sizing of the HES is built based on minimizing the CoE and the *LOLP*. A model for each component of the HES, reliability analysis, and CoE methodology, and DR strategy is introduced. A novel technique is used for the sizing of the HES components using the concepts of a smart grid. A novel DR with a dynamic tariff strategy has been used in the sizing stage to control the load based on the SoC and the charging/discharging power from the battery. The novel DR strategy uses a smart technique to predict the suitable change of cost for the situation of the battery storage system. This novel DR strategy increases the tariff when the

generation from RES is lower than the load requirements to encourage the customers to reduce their loads to maintain the HES stability. Similarly, the novel DR strategy reduces the tariff when the generation from the renewable sources is higher than the load requirements to give incentives to the customer to increase their loads to preserve the stability of the HES. This novel DR strategy reduces the sizes of HES components, reduces the capital cost of the HES, and reduces the CoE substantially. The optimal size of each component of the proposed model is determined using the PSO technique for lower cost and highest or reasonable reliability. The results obtained from PSO are compared with the results obtained from BA and Social mimic optimization, SMO [34]. The results obtained from the optimization process prove the superiority of the novel DR introduced in this article in reducing the CoE of the HES by 20.66% compared to the results obtained from the conventional sizing strategy.

The rest of this article is designed to show the SGC in section II. The novel demand response strategy is introduced and discussed in section III. The modeling of the HES components based on SGC is shown in section IV. The PSO, BA, and SMO optimization techniques are introduced in section V. The proposed sizing program based on smart grid is shown in section VI. The simulation results are shown in section VII. The conclusions and future work are shown in section VIII.

II. SMART GRID CONCEPTS
Due to the intermittent nature of the RES, it is not having a considerable penetration in the power systems. These sources need a storage system and/or fossil fuels power plants to increase their penetration. The use of the SGC can increase the penetrations of the RES in the modern power system, where it is possible to control the load to have a correlation between the generation from RES and the load. With the use of SGC the power system can work securely, efficiently, economically, and environmental friendly [35], [36]. Demand Response (DR) as one of the SGC is used widely to share the responsibility of the stability of the power system between the system operators and the customers. Where the DR strategies can induce the customers to reduce or increase their loads when required the load is greater than the generation or the load is lower than the generation, respectively [37]. The smart grid is using smart communication technologies and smart measurement devices to manage the operation of the power system and enhance the stability of the power system through controlling the load demand to be correlated with the available generations [38], as shown in Figure 1.

A. DEMAND SIDE MANAGEMENT STRATEGIES
The idea of using the smart grid system is to share the responsibilities between the customers and the electricity providers where the customer can know the situation of the smart grid system. The two-way control of the load can be accomplished in the smart grid in two different categories. The first one is the ability of the smart grid system operator to switch on/off or control its operation some loads that can be controlled
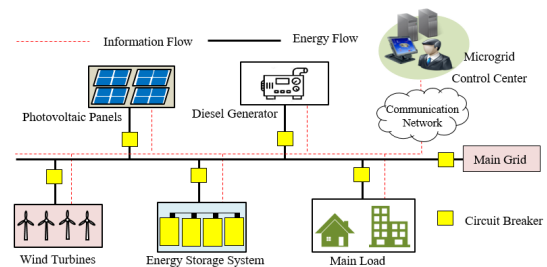

FIGURE 1. Overview of a smart grid system with hybrid renewable energy.
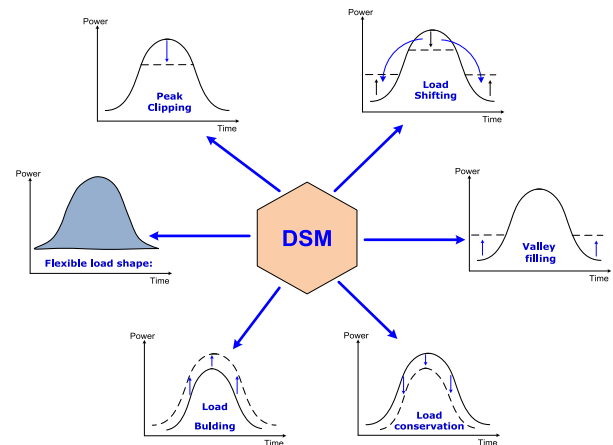

FIGURE 2. Demand-side management strategies.

without affecting its normal operations like desalination stations if the tank of the freshwater is almost full or the control the siting temperature of air conditions of some big loads. The other load control can be accomplished by using demand-side management (DSM) strategies. The function of the DSM is simply to balance the value of the load with the available generation from the smart grid system. Many DSM strategies can be used to overcome the peak load periods as shown in Figure 2. These strategies are summarized in the following points:

Peak clipping: This strategy is used when the capacity of the smart grid cannot fulfill the loads during the peak periods. In this case, the smart grid can do many actions like switching off some loads that able to be switched off for the period of the peak, or the energy price (Electricity tariff) can be increased to encourage the customer to reduce their loads.

Valley filling: This strategy is used to increase the loads in the low load periods when the generation is greater than the loads. This strategy can be accomplished by switching on low important loads and by reducing the energy price (Electricity tariff) to incentive the customers to increase their loads.

Load shifting: The load shedding strategy is used to move the low priority loads during the peak periods to the valley periods to increase the load factor of the load curve and overcome the critical periods of peaks and fill the valleys. This technique can be accomplished by switching of the low priority loads and switch them on again at the valley periods or it can be accomplished by increasing the price of
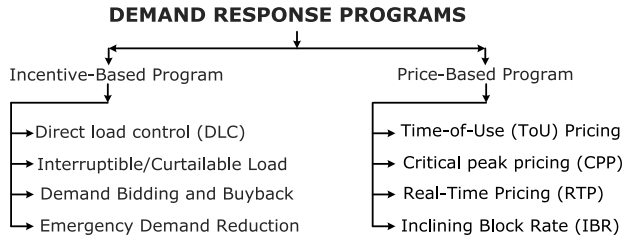
DEMAND RESPONSE PROGRAMS

Incentive-Based Program   Price-Based Program

- Direct load control (DLC)
- Interruptible/Curtailable Load
- Demand Bidding and Buyback
- Emergency Demand Reduction

- Time-of-Use (ToU) Pricing
- Critical peak pricing (CPP)
- Real-Time Pricing (RTP)
- Inclining Block Rate (IBR)

FIGURE 3. The demand response programs classifications.

FIGURE 4. The price-based demand response programs.

energy (Electricity tariff) during the peak periods and reduce it during the valley.

Flexible load shape: This sometimes called dynamic load management in which the load is controlled based on the current situation of the generation. This strategy can be accomplished by using a dynamic electricity tariff.

Load conservation: This strategy is sometimes called load reduction in which the load is required to be reduced all over the load period. This can be accomplished by switching of unimportant loads or increasing the electricity tariff.

Load building: This strategy is used to increase the load all over the load period due to the generation is greater than the load and the increase in the load is to maintain the stability of the smart grid system. This can be accomplished by increasing the electricity tariff.

B. DEMAND RESPONSE PROGRAMS

Demand response implies that the response of customers to the incentives or penalties that the electric utility takes to encourage the customer to do some actions. These programs are introduced to shape the loads to correlate with the generation available and reduce the need for installing new generation power plants to face the peak periods. There are two main categories of demand response programs (DRP) which are the incentives-based programs and the price-based programs [39]. The classification of the DRP is shown in Figure 3 and shown in details in the following:

1) INCENTIVE-BASED PROGRAM

This DRP is based on providing the customers some incentive when they reduce their loads during the peak period not based on electricity price. The incentive-based program is further classified to:

Direct load control (DLC): In this DRP, the customers give the utility operators permission to switch on/off certain loads based on their need. These loads can be desalination stations, air conditions, etc. The utility operators use these loads to reduce the peak demand at peak periods and dispatch it during curve valleys to preserve the stability of the power system.

Interruptible/Curtailable Load: The idea of this DRP is to permit the utility to reduce your load during the critical peak periods and they give the customers some incentive discount on electricity bills in return [40].

Demand Bidding and Buyback: This DRP is discussed in detail in [41], in this DRP the customers can benefit from cost-saving if they are accep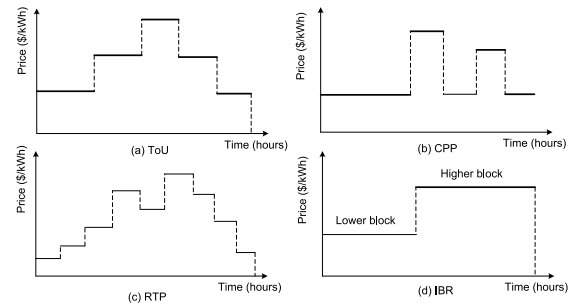ting to reduce their loads at a specific bid price. This DRP is used with big customers and it is used only with wholesale price.

Emergency Demand Reduction: This DRP is discussed in detail in [42] which the customers can get some rewards or incentives if they could reduce their loads based on short notice in case of emergency. Also, this DRP is used with big customers.

2) PRICE-BASED PROGRAM

The other DRP is done by using a variable tariff to improve the load curve and to reduce the loads during critical peak periods and to fill the valleys. The change of the tariff is used to induces the customers to cooperate with the real situation of the electric power system. Many programs issued for this purpose and some of these programs are shown in Figure 4 and listed in the following points:

Time-of-Use (ToU) Pricing: This DRP is using a predefined tariff for each period during the day, a week, month, or a season. In this DRP, the electricity providers give the price plan to the customer at the beginning of the contract based on the data available for the energy providers about the critical peak periods and valleys and their correlations with the generation available.

Critical peak pricing (CPP): This DRP is using a fixed tariff during the most period of time but it gives only high prices for a certain hour/hours during the day and it is used only for several numbers of days during the year and it has a relation on the seasonal activities of the customers during these periods and it can be changed based on the change of the behavior of the loads and generations [43].

Real-Time Pricing (RTP): This type of DRP is the most important one and it is used widely in smart grid systems and it will be used in the sizing of the proposed HES of this article. This DRP is sometimes called dynamic tariff in which the tariff is changing every certain short period maybe each hour or even each 15 min. The change of the electricity price may be based on the frequency regulation in the large power system or it may be based on the state of charge (SoC) of the battery in micro-grids or autonomous hybrid power systems. The reduction of SoC of the battery in autonomous HES indicates the loads are greater than the available generations. This DRP is very helpful for small HES that mainly depend on renewable resources like wind and PV
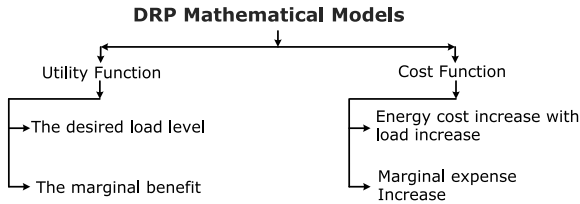
DRP Mathematical Models

Utility Function

→ The desired load level

→ The marginal benefit

Cost Function

→ Energy cost increase with load increase

→ Marginal expense Increase

FIGURE 5. Classifications of the DRP mathematical models.

that have an intermittence nature and for this reason an active collaboration between the customers and smart grid operators is very important to preserve the stability of the smart grid in abnormal conditions.

Inclining Block Rate (IBR): This DRP is using two or more levels of price for the customers based on their amount of energy they used during the month. The customers' used a small amount of energy will pay a lower price of electricity and vice versa which is using in Saudi Arabia and many other countries. This DRP is discussed in detail in [44] and it has been widely adopted by many power utilities since the 1980s [39].

C. DEMAND RESPONSE MATHEMATICAL MODELS
Several techniques have been introduced in the literature to model the DRP used to control the loads to correlate with the available generations. These DRP mathematical models are classified in Figure 5 and they are defined in the following points:

Utility Function: Different choices of utility functions will be chosen to model the behaviors of customers. More formally, the utility represents the level of comfort/satisfaction obtained by the user as a function of his/her energy consumption, which is non-decreasing and concave. The quadratic utility functions are usually considered, which correspond to two linear decreasing marginal benefits. A detailed description of this model is introduced in [45], [46]. This model can be further classified to the desired load level and marginal benefits models [39]. The desired load level model is based on the customers with high power should restrict following the smart grid operators to preserve the desired load level. The marginal benefit is by using a concave function which makes the customers feel comfortable when their energy consumption gets their satisfaction.

Cost Function: The cost function is used to model the cost of generating electricity in convex shape. The cost function model is further classified as shown in Figure 5 to energy cost increase with load increase, and marginal expense increase. A detailed description of these models is shown in [47], and [48].

III. THE NOVEL DEMAND RESPONSE STRATEGY
In this article, a novel adaptive DR strategy is introduced. The tariff is changing based on the SoC and the charging/discharging power of the battery. This strategy detects the SoC of the battery to change the tariff. Where the reduction in the SoC means that the loads are greater than generations
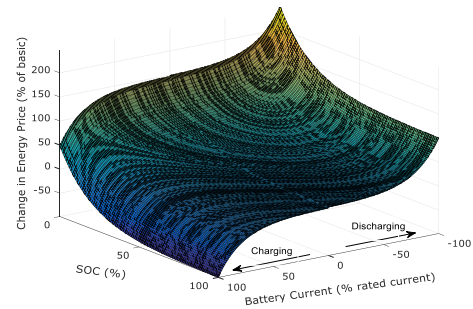

FIGURE 6. The new proposed DR program, $\alpha_1 = 0.05$ and $\alpha_2 = 0.046$.

and the tariff should be increased and vice versa. This strategy suggested continuously tariff increase until the generation/load balance is reached. Otherwise, the required value and the energy of the battery becomes near to its lower SoC limit, the Diesel generator should be started to feed the load during these conditions. On the other hand, in case of the generation from RES is greater than the load and the battery is full, an incentives program should be added to the customers to encourage them to increase their loads by reducing the tariff, otherwise the surplus energy should be transferred to dummy loads. The new relation governing the new DR is shown in equation (1) and the 3-D plot showing this strategy is shown in Figure 6. The new tariff in terms of the tariff of the previous step $p_r(t-1)$ and the change in tarif based $\Delta p_r(t)$ is shown in equation (1).

$$\Delta p_r(t) = e^{\alpha_1(100-SoC(t))} \pm e^{\alpha_2 * |P_B(t)/P_{BR}|} \qquad (1)$$

Discharging

Charging

where, $P_B(t)$ and P_{BR} are the hourly and rated battery power. The factors α_1 and α_2 are numerical coefficients with values equal to 0.05 and 0.046, respectively, these values of coefficients (α_1 and α_2) can be adjusted based on the DR history of the smart grid in each site. The new tariff can be obtained as shown in (2).

$$p_r(t) = p_r(t-1) * (1 + \Delta p_r(t)/100) \qquad (2)$$

A. PRICE ELASTICITY OF DEMAND (PED)
The relation between the percentage change in tariff, $\Delta p_r(t)$ and the percentage change in load is called the price elasticity of demand (*PED*) and it can be represented as shown in equation (3) [49]. The shape of the curve depends mainly on many social and economic issues and it has been introduced in many studies as a linear relationship as shown in Figure 7 [49]. In the case of *PED* higher than -1 (between 0 and -1) it means that the *PED* has low elasticity (Inelastic), meanwhile, if *PED* < -1, it means that the load has high elasticity (Elastic). In the case of the *PED* is equal to -1 it called the *PED* is unitary. In this study, the *PED* has been selected with different values to see the effect of the value of *PED* on the CoE of the HES and other parameters of the HES. Figure 8 shows the relation between the change in tariff
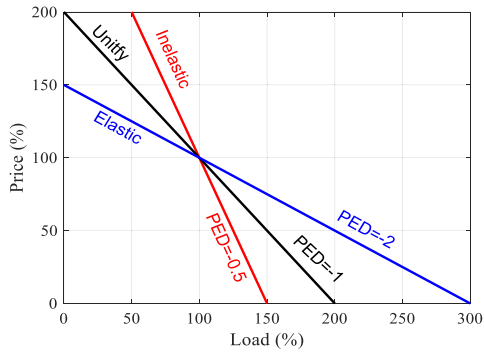
FIGURE 7. The relation between the price and load demand in different DR scenarios.
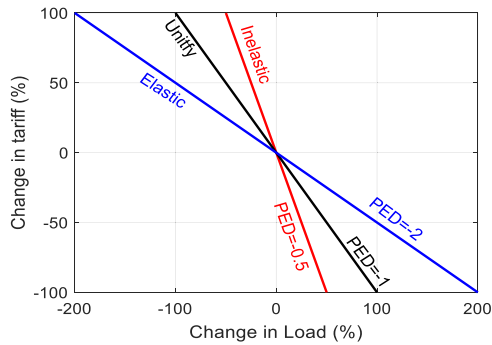

FIGURE 8. The relation between the change in price and the change in load For PED = −0.5, −1.0. −2.0.

and the change in load For $PED = -0.5, -1.0. -2.0$ as an example.

$$PED = \frac{\Delta P_L / P_{L0}}{\Delta p_r / p_{r0}} \quad (3)$$

where, the ΔP_L and Δp_r are the percentage change in power and price of energy, respectively. The value of PED should be a negative value where when the change in price is positive, the change in load should be negative and vice versa.

IV. MODELING OF HES BASED ON SMART GRID CONCEPTS

The proposed HES is consisting of a WES, PV energy system (PVES), battery, DE, loads, and the power electronics converter as shown in Figure 9. The WES used in this study generates AC power and for this reason it is economically to connect it with the AC bus.

Most of the autonomous HES are usually use RES like WES and PVES that have intermittent nature of their generated power which need a battery to save the energy during the generation is greater than the load requirements. Moreover, a DE is used to give extra power in case of the battery is not able to supply the load. The idea of using the battery as a first backup because of its fast response and its lower operating cost in low power use is shown in Figure 10 [50].

A. MODELING OF THE HES COMPONENTS

In the energy balance program, the generated energy from the WES, PVES, DE, and the performance of the battery system
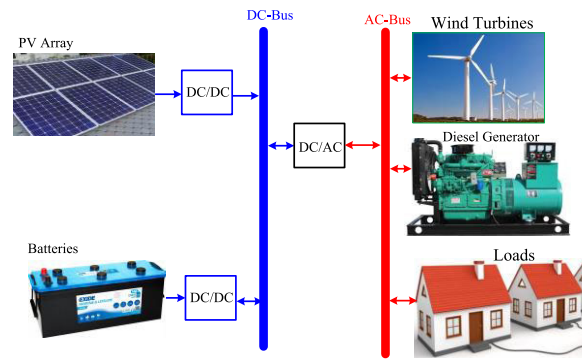

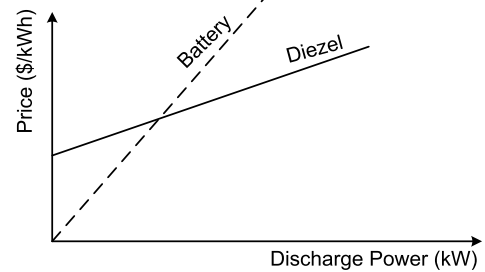**FIGURE 9.** The configuration of the HES.

FIGURE 10. The cost comparison between the use of battery and Diesel for certain HES [50].

and power electronic converter is determined. The model of each component is used to determine its performance on different operating conditions as shown in the following:

1) WIND ENERGY SYSTEM MODEL
The measurements of wind speeds are performed at the height of the anemometer which should be modified to the height of the wind turbine. The relation between the wind speed to any height, h, and the anemometer height is shown in equation (4) [2].

$$u(h) = u(hg) * \left(\frac{h}{hg}\right)^{\alpha} \quad (4)$$

$$P_w(v) = \begin{cases} 0 & U_C \& u \geq U_F \\ P_R * \dfrac{u^k - U_C^k}{U_R^k - U_C^k}, & U_C \leq u \leq U_R \\ P_R & U_R \leq u \leq U_F \end{cases} \quad (5)$$

where, U_C, U_R, and U_F are the WT cut-in speed, rated speed, and cutoff speed, respectively.

2) PV ENERGY SYSTEM MODEL
The generated electric power from the PVES is affected substantially by the irradiance falling on the PV as well as its area. To increase the irradiance and consequently the generated energy from the PV system it is recommended to tilt the PV modules with an optimal tilt angle. This optimal tilt angle is chosen to be equal to the latitude angle of the site [2]. The hourly generated power from the PV array can be determined by the following equation:

$$P_{PV}(t) = H_t(t) * PVA * \eta_c(t) \quad (6)$$

where, H_t is the solar radiation on an optimally tilted surface, *PVA* is the total area of PV array, and $\eta_c(t)$ is the hourly efficiency of PV array which can be obtained by the following equation [2]:

$$\eta_c(t) = \eta_{cr}[1 - \beta_t \times (T_c(t) - T_{cr})] \quad (7)$$

where, β_t is the temperature coefficient and its value used in this study is 0.005 per °C [51], T_{cr} and η_{cr} are the solar cell temperature and efficiency, respectively. $T_c(t)$ is the instantaneous solar cell temperature at the ambient temperature (T_a) which can be obtained by the following equation:

$$T_c(t) = T_a + 3H_t(t) \quad (8)$$

3) BATTERY STORAGE MODEL
During the operation of the battery, it loses some of its charges whenever it is charging, discharging, or storing. The factor that characterizes the loss of its energy is called the self-discharge rate. The equation that shows the SoC of the battery due to the self-discharge rate (SDR) is given by the following equation [52]:

$$E_B(t+1) = E_B(t)(1 - \sigma) \quad (9)$$
$$E_{B,min} \leq E_B(t) \leq E_{B,max} \quad (10)$$
$$E_{B,min} = (1 - DoD) \quad E_{BR} \quad (11)$$

4) DIESEL GENERATOR MODEL
The diesel generator is representing a backup when the battery cannot fulfill the deficit power. The function used to determine the fuel consumption of the Diesel engine (L/kWh) is shown in equation (12) [54].

$$FD = 0.08415P_{dsr} + 0.246P_{ds}(t) \quad (12)$$

where P_{dsr} is the rated power of Diesel generator and $P_{ds}(t)$ is the generated power at time t. In this article, the minimum allowable load ratio is 30% [54]. The fuel cost is \$0.9/L [55].

B. RELIABILITY INDICES
The technical objectives used in the sizing of the HES are mainly the reliability indices that are shown in the following points:

Loss of load expected (LOLE): *LOLE* is defined as the total number of hours for which the HES is not able to provide the load with its need. This factor accumulates the number of hours that the HES cannot afford the required power by the loads during the total number of hours of complete one year (8760 hrs). The *LOLE* is shown in (13) [56], [57].

$$LOLE = \sum_{i=1}^{8760} t_{outage}(i) \quad (13)$$

where, t_{outage} is the hour that the loads can be supplied by the HES and its value =1 in case of the loads cannot be served otherwise it equals zero.

Loss of load probabilities (LOLP): This factor is defined as the ratio between the *LOLE* and the total number of hours

of complete one year (8760 hrs). The relation showing the value of the *LOLP* and its relation with the *LOLE* is shown in (14) [56], [57].

$$LOLP = \frac{\sum_{i=1}^{8760} t_{outage}(i)}{8760} = \frac{LOLE}{8760} \quad (14)$$

Level of autonomy (LA): *LA* is representing the ratio between the hours that the HES can feed the load efficiently to the total number of hours which can be obtained in the following equation:

$$LA = 1 - LOLP = 1 - \frac{\sum_{i=1}^{8760} t_{outage}(i)}{8760} = 1 - \frac{LOLE}{8760} \quad (15)$$

Expected energy not supplied (EENS): *EENS* is representing the total amount of energy that the HES cannot serve during yearly and it can be obtained from the following equation:

$$EENS = \sum_{i=1}^{8760} P_L(i) - P_{H,max}(i) \quad \forall P_L(i) > P_{H,max}(i) \quad (16)$$

Loss of energy expected (LOEE): This factor is used to measure the ratio of the amount of energy that the HES cannot supply to the load to the total energy load. This index is sometimes called loss of power supply probability (*LPSP*). This can be obtained by accumulating the amount of energy not supplied divided by the total energy supplied to the load. It worth to be noted that some other researchers used the *LPSP* to represent the *LOLP* as shown in (17) [58], and [15].

$$LOEE = \frac{\sum_{i=1}^{8760} P_{de}(i)}{\sum_{i=1}^{8760} P_L(i)} \quad (17)$$

where, $P_{de}(t)$ is the difference in power from the load and the maximum power afforded from the HES and it can be obtained from the following equation:

$$P_{de}(i) = P_L(i) - P_{H,max}(i) \quad \forall P_L(i) > P_{H,max}(i) \quad (18)$$

Equivalent loss factor (ELF): This factor is used to get the summation of the ratios of power did not cover by the HES to the load power at time t, divided by the total number of steps the reliability index is used (8760 hrs) in this study. This index can be obtained as shown in the following equation [58]:

$$ELF = \sum_{i=1}^{8760} \frac{P_{de}(i)}{P_L(i)} \quad (19)$$

Renewable energy fraction (REF): *REF* is representing the total energy delivered to the load from RES to the load

demand as shown in the following equation:

$$REF = \left(1 - \frac{\sum\limits_{t=1}^{8760} P_{ds}(t)}{\sum\limits_{t=1}^{8760} P_L(t)}\right)^* 100 \qquad (20)$$

where $P_{ds}(t)$ is the generated power from the Diesel generator at time t.

C. THE POWER DISPATCH

The power dispatch is divided into two operating conditions. The first one is when the generation is lower than the load and the second one is when the generation is higher than the load. These two operating conditions are shown in detail in the following points and shown in detail in Figure 11.
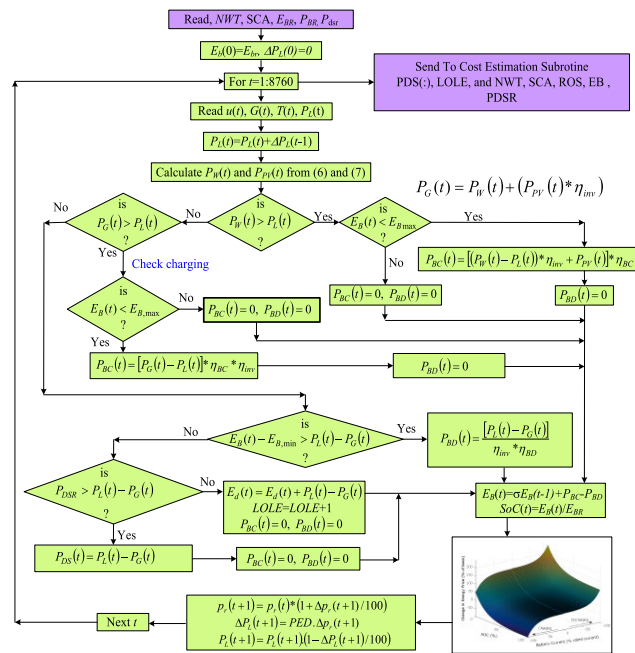

FIGURE 11. The power dispatch subroutine.

1) THE GENERATION IS LOWER THAN THE LOAD

The logic used in this part is built on using the battery to feed the load whenever the stored energy in the battery is adequate to feed it. If it is not enough to feed the load, the DE should work to feed the load in case of the defect power is greater than the minimum allowable load ratio is 30% [54]. In case of the deficit, power is less than 30% the DE will be used to charge the battery with the rest of this percentage.

In case of the DE is not able to satisfy the load requirements a case of *LOLP* condition is occurred. The mathematical model showing this logic is shown in the following equation:

If $P_G(t) < P_L(t)$ and $E_B(t) - E_{B,\min} > P_L(t) - P_G(t)$

Then, the power discharged from the battery is as shown in the following equation:

$$P_{BD}(t) = \frac{[P_L(t) - P_G(t)]}{\eta_{inv}\,\eta_{BD}} \qquad (21)$$

where,

$$P_G(t) = P_W(t) + (P_{PV}(t)\,\eta_{inv}) \qquad (22)$$

The stored energy of the battery that will be used in the next step is shown in the following:

$$E_B(t+1) = E_B(t+1) - P_{BD}(t) \qquad (23)$$

The *SoC* of the battery is the percentage of total stored energy after this step which can be obtained by dividing the current energy of the battery by the rated energy of the batteries (E_{Br}) which can be obtained from the following equation:

$$SoC(i+1) = E_B(i+1)/E_{Br} \qquad (24)$$

If the generated power from RES ($P_G(t)$) is lower than the load demands $P_G(t) < P_L(t)$ and the stored energy in the battery is lower than the loads need, $E_B(i) - E_{B,\min} < P_L(i) - P_G(i)$, then the Diesel generator should start to feed the deficit as shown in the following equation:

$$P_{ds}(t) = P_L(t) - P_G(t) \qquad (25)$$

In case of the $P_{ds}(t) < 0.3^*P_{dsr}$, then the rest of this percentage will go to charge the battery as shown in the following equation:

$$P_{BC}(t) = 0.3^*P_{dsr} - P_{ds}(t) \qquad (26)$$

If the required power from the Diesel generator is greater than its rated power, $P_L(t) - P_G(t) > P_{dsr}$, then the loss of load expected (*LOLE*) will be increased by one occurrence as shown in equation (27). Also, in this case, the loss of energy expected (*LOEE*) can be obtained from equation (28).

$$LOLE = LOLE + 1 \qquad (27)$$

$$LOEE = LOEE + \frac{P_L(i) - P_G(i) - P_{dsr}}{\sum\limits_{t=1}^{8760} P_L(t)} \qquad (28)$$

In this case, the accumulated deficit in the generated energy, E_d can be obtained as shown in the following equation:

$$Ed = Ed + P_L(t) - P_G(t) - P_{dsr} \qquad (29)$$

After finishing the above logic, the battery state of charge should also be reduced by the battery self-discharge rate, σ % of its capacity every one hour during the simulation where the state of charge can be extracted from (30).

$$E_B(t) = \sigma E_B(t-1) \qquad (30)$$

The new *SoC* obtained above and the deficit power should be used to determine the percentage change in price as shown in the following equation:

$$\Delta p_r(t+1) = e^{0.05(100 - SoC(t))} + e^{0.046^*|(P_L(t) - P_G(t))/P_{BR}|} \qquad (31)$$

The new price of energy per kWh can be obtained from the following equation:

$$p_r(t + 1) = p_{rb} \cdot [1 + \Delta p_r(t + 1)/100] \qquad (32)$$

where, p_{rb} is the basic price of the energy per kWh, P_{BR} is the rated power from the battery.

The load reduction due to the DR of the next hour can be obtained from the following equation:

$$P_L(t+1) = P_L(t+1) \cdot (1 - PED \cdot \Delta p_r(t + 1)) \qquad (33)$$

where, *PED* is the price elasticity of demand.

2) THE GENERATION IS GREATER THAN THE LOAD

In the case of the generation from the RES (the wind turbines and the PV array) is greater than the load, the extra power should go to charge the battery otherwise it will go to the dummy loads.

At the beginning of this operating condition, the logic should check first if the generated energy is greater than the load requirements if $P_G(t) > P_L(t)$, then the logic should go to check first if the generation from the wind turbines is adequate to feed the load requirements alone to feed the load from wind turbines and the rest with the PV output will go to charge the battery. The idea behind feeding the load from wind turbines only is because its output is AC which is suitable for the load and we do not need to convert the DC output power from the PV through the inverter to the load which can lose a considerable amount of power in the losses of the inverter. This logic is shown in the following equations:

If $P_W(t) > P_L(t)$ and $E_B(t) < E_{B,\max}$, then the surplus power will charge the battery by $P_{BC}(t)$ as shown in equation (34); meanwhile the discharging power from the battery, $P_{BD}(t)$ is zero.

$$P_{BC}(t) = [(P_W(t) - P_L(t)) \, \eta_{inv} + P_{PV}(t)] \, \eta_{BC} \quad (34)$$

The new stored energy in the battery is shown in (35) and the new *SoC* can be obtained from (36).

$$E_B(t + 1) = E_B(t + 1) + P_{BC}(t) \qquad (35)$$
$$SoC(t + 1) = E_B(t + 1)/E_{Br} \qquad (36)$$

If $P_W(t) > P_L(t)$ and $E_B(t) \geq E_{B,\max}$, then the battery will not able to get extra energy and the control system will get rid of the extra power to the dummy loads as shown in (37) and the charging/discharging power to the battery can be obtained from (38).

$$P_{dummy}(t) = (P_W(t) - P_L(t)) + P_{PV}(t) \cdot \eta_{inv} \quad (37)$$
$$P_{BC}(t) = P_{BD}(t) = 0 \qquad (38)$$

If $P_W(t) < P_L(t)$, meanwhile $[P_W(t) + (P_{PV}(t)) \, \eta_{inv}] > P_L(t)$ and the batteries are not fully charged, $E_B(t) < E_{B,\max}$, then the extra power will be transferred to charge the batteries as shown in the following equation:

$$P_{BC}(t) = [P_W(t) + (P_{PV}(t) \, \eta_{inv}) - P_L] \, \eta_{BC} \quad (39)$$

If $P_W(t) < P_L(t)$, meanwhile $[P_W(t) + (P_{PV}(t) \, \eta_{inv})] > P_{RO}(t)$ and $E_B(t) \geq E_{B,\max}$ then the control system will discard the extra power to the dummy load, and for this reason, the charging/discharging power of the battery will be zero as shown in (40) and the power to the dummy load can be obtained from (41).

$$P_{BC}(t) = P_{BD}(t) = 0 \qquad (40)$$
$$P_{dummy}(t) = P_W(t) + P_{PV}(t) \cdot \eta_{inv} - P_L(t) \quad (41)$$

The energy to the dummy loads can be obtained by adding the new value of dummy power to the previous values as shown in (42).

$$E_{dummy} = E_{dummy} + P_{dummy}(t) \qquad (42)$$

After finishing the above logic, the battery state of charge should also be reduced by the battery self-discharge rate, σ % of its capacity every one hour during the simulation where the state of charge can be extracted from (43).

$$E_B(t) = \sigma \, E_B(t - 1) \qquad (43)$$

The new SoC obtained above and the surplus power should be used to determine the percentage change (reduction) in price as shown in the following equation:

$$\Delta p_r(t + 1) = e^{0.05(100 - SoC(t))} - e^{0.046 * |(P_G(t) - P_L(t))/P_{BR}|} \qquad (44)$$

The new price of energy per kWh can be obtained from the following equation:

$$p_r(t + 1) = p_{rb} \cdot [1 + \Delta p_r(t + 1)/100] \qquad (45)$$

where, p_{rb} is the basic price of the energy per kWh, P_{BR} is rated power from the battery.

The load increase due to the DR of the next hour can be obtained from the following equation:

$$P_L(t + 1) = P_L(t + 1) \cdot (1 + PED \cdot \Delta p_r(t + 1)) \qquad (46)$$

where, *PED* is the price elasticity of demand.

D. COST ANALYSIS

The main objective of this section is to determine the *CoE* which can be obtained by using the Levelized CoE (*LCE*) factor which can be obtained from (47). In this calculation, all the factors affecting the price during the operation of the HES will be referred to the time of starting the paper taking into consideration the interest and inflation rates. The total present value (*TPV*) will be used to determine the *LCE* to better choose the best size of each component of the HES as shown in (47) [59]. Many studies introduced economical methodologies to calculate the *CoE* depending on many assumptions. The *TPV* of the system components, *OMC*, and the price of salvage parts are introduced in [60], [61]. The *TPV* is used to determine the *CoE* from HES as shown in the following equations:

$$LCE = \frac{TPV * CRF}{YE} \qquad (47)$$

where YE is the yearly generated energy from the HES, and CRF is the capital recovery factor which is shown in (48).

$$CRF = \frac{r(1+r)^T}{(1+r)^T - 1} \tag{48}$$

where; T is the paper lifetimes in years, and r is the net interest rate.

The value of TPV can be determined from (49).

$$TPV = CC + RC + OMC - PSV \tag{49}$$

where CC is the capital cost of the whole system including the installation cost, RC is the replacement cost, OMC is the operation and maintenance cost, and PSV is the present value of the salvage [59]. The detailed descriptions of the variables shown in (49) are shown in the following sections:

1) CAPITAL COST
The capital cost (CC) of the HES systems including the price of all parts of the system, the installation cost, and etc. which can be calculated as shown in (50).

$$CC = WEp + PVp + BAp + DGp + SGp \tag{50}$$

where, WEp is the price of wind energy system including installation, power electronics conditioners, and price of all components required for the wind energy system, PVp is the total price of PV energy system including the installation, civil work, power electronics conditioner, and control system. BAp is the total price of the battery system with the all required components for this system. DGp is the total price of the Diesel generator price. SGp is the total price of sensors, communication systems, and the control center of the smart grid which has been used as 5% of the cost of the other components.

2) REPLACEMENT COST
The components that have a lifetime less than the lifetime of the paper should be replaced during the operation of the paper. These replaced components will be bought at the time of the replacement. The cost of these components should be calculated as a present value when the paper started taking into consideration the interest rate, r, and inflation rate, l. The cost of replacement of any component of the system at the beginning of the paper, RC is shown in equation (51) [52].

$$RC = RCU \sum_{j=1}^{N_{rep}} \left(\left(\frac{1+l}{1+r} \right)^{T*j/(N_{rep}+1)} \right) \tag{51}$$

where, RCU is the current replacement cost of the components that will be replaced during the paper period, N_{rep} is representing the times that the component is replaced during the lifetime of the paper, T.

3) OPERATION AND MAINTENANCE COST
The proposed system needs an OMC during the lifetime of the paper. There is no exact evaluation for the OMC for each price but the value used for it is obtained from experts and previous research work or as recommended by the manufactures of the components. These values will be shown in detail in the simulation section.

The present value of OMC of any component in the HES can be determined from (52) [52]:

$$OMC = OMC_0 * \left(\frac{1+l}{r-l} \right) * \left(1 - \left(\frac{1+l}{1+r} \right)^T \right), \quad r \neq l \tag{52}$$

4) THE PRESENT SALVAGE VALUE
The old components that are replaced with new ones during the operation of the paper will be sold at the time of replacement. The values of these components should be calculated at the starting of the paper which is called the PSV which can be calculated as shown in equation (53) [52].

$$PSV = \sum_{j=1}^{N_{rep}+1} SV * \left(\frac{1+i}{1+r} \right)^{T*j/(N_{rep}+1)} \tag{53}$$

where SV is the scrap or salvage value.

V. OPTIMIZATION TECHNIQUES
Three swarm optimization techniques have been used for getting the optimal sizing of the components of the HES and the CoE taking into consideration the DR as a smart grid concept. These three optimization techniques introduced in this article are chosen with two well know techniques and one recently introduced optimization technique. The three techniques are, the BA [62], the PSO [15], and the social mimic optimization, SMO [34] algorithms. The optimization used multiobjective function to minimize both the CoE, and the $LOLE$ values as shown in (54).

$$F = M * LCE + LOLE \tag{54}$$

where, F is the objective function, LCE is the Levelized CoE, and M is the weight value to give the $LOLE$ the required weight compared to LCE.

A. OPTIMIZATION TECHNIQUES INITIALIZATION
In the beginning (initialization) of all optimization techniques used in this study, the values of optimization variables (NWT, SCA, E_{BR}, and P_{dsr}) with numbers of particles called swarm size, n. The initial values in the original optimization techniques are recommended to be random, but random values of these variables, may increase the convergence time and may cause the premature convergence. So, it is recommended to have random values within reasonable limits of these variables. The initial values of NWT, PVA, E_{BR}, and P_{dsr} will be fed to the energy balance and cost estimation subroutines and the values of the objective function shown in (54) will be collected, $F_0^{1:n}$. The minimum value of the objective function will be determined as $F_{best} = \min(F_0^{1:n})$ and the corresponding best bat, d_{best} will be determined.

B. THE PSO IN SIZING OF THE HES

The PSO technique is a very popular optimization technique where it has been used in numerous applications. This technique imitates the behaviour of many flocks of animals like fish or birds in searching for their food to use the same searching technique in capturing the optimal solutions of real-world applications. This technique is introduced in 1995 by Kennedy and Eberhart (1995) [63]. The idea behind this technique is sending many searching agents called the swarm and each one is called a particle to search for the optimal solution. The experience gained from the searching step will be transferred to offspring in the next step. The particles share their experience among the other particles in the swarm (social-experience) and use their private experience (self-experience) to modify the searching technique.

The searching performance of the PSO is performed using two equations (55) and (56). The first equation is used to determine the velocity or trajectory of particles in the new iterations v_{i+1}^k. The velocity of the particles in the next step $v_{i+1}^{1:n}$ is obtained from three different terms which are summarized in the following points:

- The previous velocity $v_i^{1:n}$ is multiplied by the weight function ω to enhance the stability of searching performance [64].
- The second term is using the difference between the particle's best value and the current solution and multiplies this difference by a factor called self-experience parameter, c_l. increasing the value of this parameter will enhance the self-confidence of searching and it increases the convergence speed but it may increase the possibility of capturing a local peak.
- The third term is the difference between the global best obtained from the previous iteration and the current solution and multiplies this difference by a factor called social-experience parameter, c_g. increasing the value of this parameter will enhance the social-confidence of searching.

The values of c_l and c_g should be compromised to balance between the self and social search which differ from one fitness function to another. This velocity or trajectory will be added to the previous position of particles $d_i^{1:n}$ to get the new values of particles [65]. The flowchart showing the logic used in the optimal sizing of HES by PSO is shown in Figure. 12.

$$v_{i+1}^{1:n} = \omega v_i^{1:n} + c_l r_l (d_{best}^{1:n} - d_i^{1:n}) + c_g r_g (G_{best} - d_i^{1:n}) \quad (55)$$

$$d_{i+1}^k = d_i^k + v_{i+1}^k, \quad (56)$$

where, ω is called the inertia weight, c_l and c_g are the self and social experience parameters, respectively. $d_{best}^{1:n}$ is the personal best position of each particle, G_{best} is the global best position, n is the number of searching agents (swarm size), and r_l and r_g are random values in between [0 1], i is the iteration order which starts at 1 to the end of iterations when $i = it$.
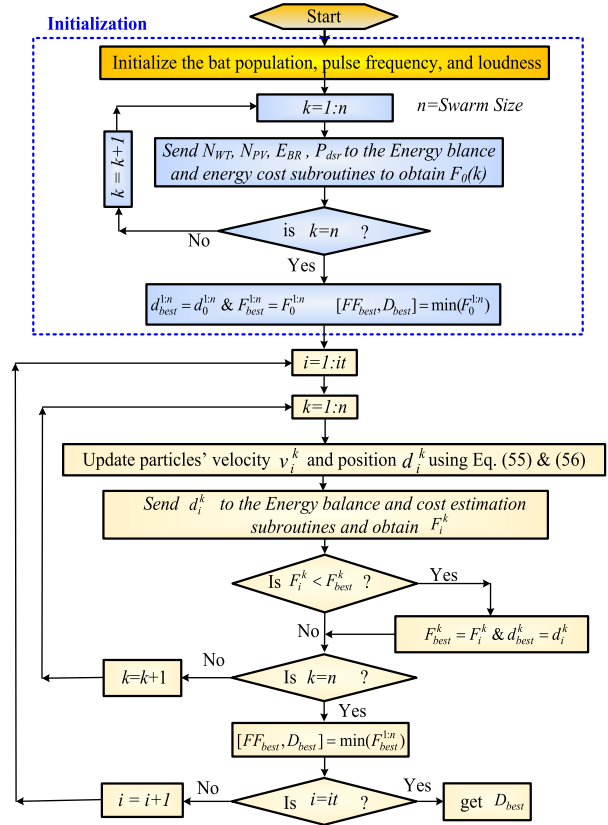

FIGURE 12. The flowchart showing the logic used in the optimal sizing of HES by PSO.

C. THE BA IN SIZING OF THE RES

Like most of the swarm optimization techniques, BA imitates the bats in searching for their food or prey. The BA is first developed in 2010 by Yang 2010 [62]. This optimization technique has very fast and accurate convergence. In nature, the bats search for their foods by using the echolocation technique in which they emit numbers of impulses with different levels and different frequencies and receive the echo of these sound pulses. The bats get information about the food or prey from the received sounds to decide their direction and speed in the next movement. The bats can identify the distance, size of the prey by measuring the time between pulses and the intensity of echoed sound pulses, respectively. The searching behavior of the bats has inspired researchers to imitate it in searching for the optimal solution for different life problems. Many generalized rules should be taken into consideration in the mathematical modeling of the BA which is shown in [62]. The following sections explain the logic of using the BA to optimally design the HES system. As with the other optimization techniques used in this article, the BA will use the number of WTs, *NWT*, The area of PV array, *SCA*, the size of the batteries, E_{BR}, and the rated power of the DE as optimization variables. The fitness function is introduced in equation (54).

The initial velocity $v_0^{1:n}$ and initial frequency $f_0^{1:n}$ of all bats are set to zero (where n is the swarm size). The initial

values of pulse rate, r_0, loudness, A_0, and many initialization parameters are set as recommended in [62].

The new position of the particles $d_i^{1:n}$ can be determined from (59) after determining the bat velocity, $v_i^{1:n}$ as shown in (58). The frequency of the particles can be determined from (57).

$$f_i^{1:n} = f_{\min} + (f_{\max} - f_{\min})\,\beta \tag{57}$$

$$v_i^{1:n} = \omega\,v_{i-1}^{1:n} + \left(d_{best} - d_{i-1}^{1:n}\right)f_i^{1:n} \tag{58}$$

$$d_i^{1:n} = d_{i-1}^{1:n} + v_i^{1:n} \tag{59}$$

where, the values of f_{min} and f_{max} is the minimum and maximum frequency range and are chosen to be 0 and 2, respectively [62]. β is a random value, $\beta \in [0, 1]$, and ω is the inertia weight.

After determining the new position from (59), a random walk around this position should be performed to get the new position of the bats as shown in (68) [66]. If the pulse emission r_i less than a random number, then the position d_i is replaced by the value obtained from (60).

$$d_i^{1:n(new)} = d_{best} + \varepsilon\phi\left\langle A_i^{1:n}\right\rangle \tag{60}$$

where, ε is a random number, $\varepsilon \in [-1, 1]$, and ϕ is a positive constant equal to 0.001 [66], while $\left\langle A_i^{1:n}\right\rangle$ is the average loudness of bats at the current iteration.

The value of loudness (A_i) decreasing with iterations meanwhile the pulse rate, r_i is increasing. The variation of A_i and r_i with iteration numbers are shown in (61) and (62), respectively [66].

$$A_i^{1:n} = \alpha A_{i-1}^{1:n} \tag{61}$$

$$r_i^{1:n} = r_0^{1:n}\left[1 - e^{(-\gamma i)}\right] \tag{62}$$

where the values of α and γ have been chosen equal to 0.9 in many types of research [66].

The new values of the bats' positions, $d_i^{1:n}$ will be fed into the fitness function (energy balance and cost estimation) to get its corresponding objective values $F_i^{1:n}$. After performing the above logic, the iterations will start and be repeated until the logic stopped using the stopping criterion. The flowchart of using BA in the design of HES is shown in Figure 13.

D. THE SMO IN SIZING OF THE RES

A modern optimization technique called the social mimic optimization algorithm (SMO) [34] is used to be compared with the PSO and BA in sizing of the HES. This algorithm is mimicking the human face and body reactions. This newly proposed technique has been used with many optimization functions and it shows good convergence performance. This technique is characterized by there is no control parameters to be optimized as in the case of the BA and PSO which makes it a good option to be used with low-experience optimization researchers. The operating logic of SMO is shown in Figure 14 and detailed in the following steps:

SMO1: The first step is to initialize the particles $d_0^{1:n}$ and then calculate the fitness function $F_0^{1:n}$.
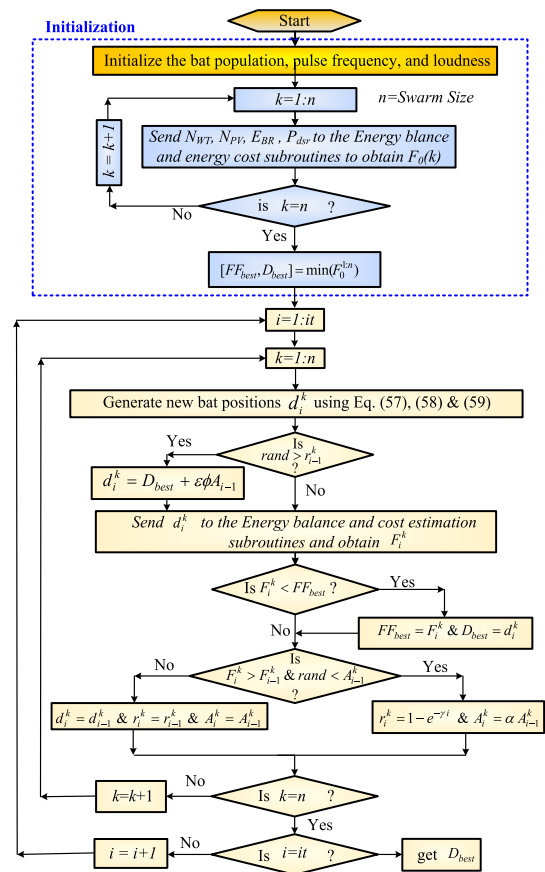

FIGURE 13. The flowchart of the Bat Algorithm used for optimal sizing of the HES.

SMO2: Determine the minimum optimization function, FF_{best} (called a leader), and set its corresponding position to d_{best}.

SMO3: Determine the difference between the value of best fitness function (leader) to the value of a function of each particle "Flower" as shown in the following equation:

$$DF_i^k = (FF_{best} - F_{i-1}^k)/F_{i-1}^k \tag{63}$$

SMO4: Check if $DF_i^k = 0$ set its value to –rand and go to the next step otherwise go to the next step.

SMO5: Determine the new position of the particles using the following equation:

$$d_i^k = d_{i-1}^k + DF_i^k \times d_{i-1}^k \tag{64}$$

SMO6: Send the new position of particles d_i^k to the EBCE and determine the corresponding fitness function F_i^k.

SMO7: Check if $F_i^k < FF_{best}$, then $FF_{best} = F_i^k$, and go to the next step, otherwise go to the next step without modification.

SMO8: Check if all particles are performed, if yes go to the next step otherwise go to SMO3.

SMO9: Check the stopping criterion is valid print the values of d_{best} and FF_{best} otherwise go to SMO3.
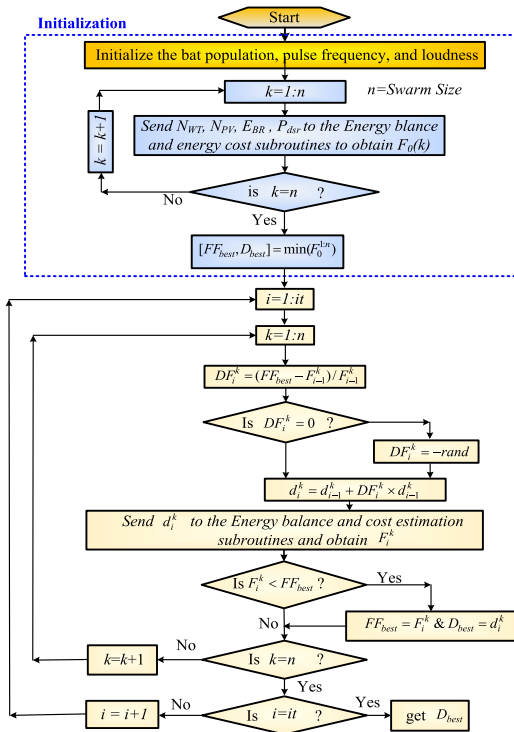
FIGURE 14. The flowchart of the SMO used for optimal sizing of HES.

VI. THE PROPOSED SIZING PROGRAM BASED ON SMART GRID

The sizing stage will carry out the above logic to imitate the real operation of the proposed smart grid operation where all the studies in the literature did not take these strategies into considerations when sizing the HES using the SGC. This strategy will help the customers to participate in the stability of the smart grid and increase the reliability of the system under all abnormal conditions. This strategy reduced the size of the components and the battery size which reduced the investments required to build the HES which can be translated into a reduction in the customer bills and an increase in energy providers profit. Suggesting to use the dynamic tariff strategy introduced in this article for the large power system is studied. This study showed the reduction in the investments used in building new big power plants and increase the dependency on renewable energy which can reduce also the customers' bills.

A. THE MAIN PROGRAM STRUCTURE

The sizing strategy used in this article is implemented in a Matlab code with structure as shown in Figure 15. The main computer program has a sequence shown in the following points and each point will be discussed in the following sections.

- Input the data and send it to different parts of the computer program.
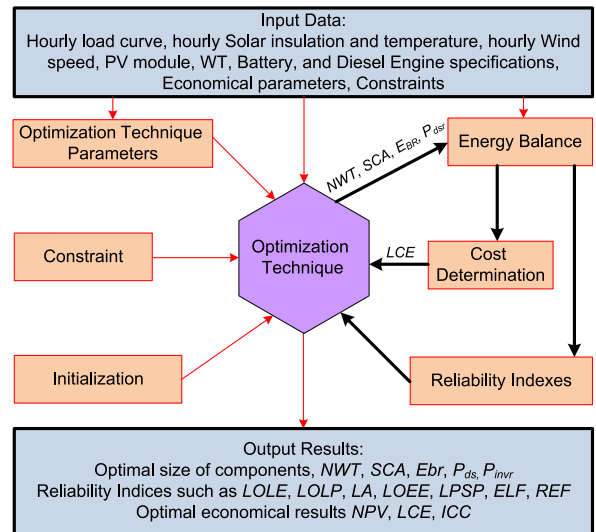- Initialize the optimization technique PSO, BA, and SMO.

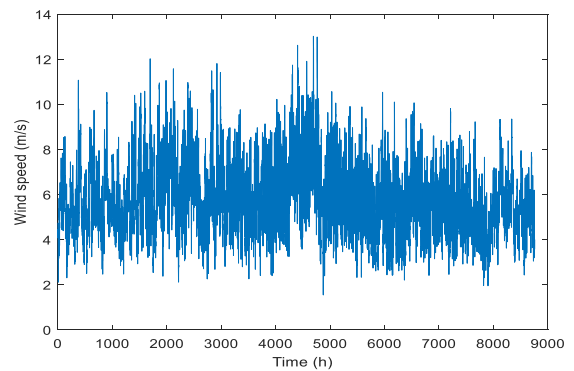**FIGURE 15.** The structure of the main computer program.

FIGURE 16. The hourly wind speed at 10 m height for Arar site.

- Send the values of searching agents from the optimization technique to the energy balance subroutine.
- Perform the energy balance between the loads and the generations taking the DR strategy into consideration and determine the total generated energy, and reliability indices like $LOLP$, $LPSP$, etc.
- Send the utilized energy, size of different HES components to the cost determination subroutine and get the Levelized CoE (LCE).
- Send the CoE and reliability indices to the optimization technique to determine the fitness value of the objective function from (54) and perform the optimization technique.
- Send the updated values of searching agents to the energy balance subroutine and continue this loop until the stopping criteria stop the optimization technique.
- Get the output results like the size of each HES component, CoE, and different reliability indices.

The details of each part of the main computer program are shown in the following sections:
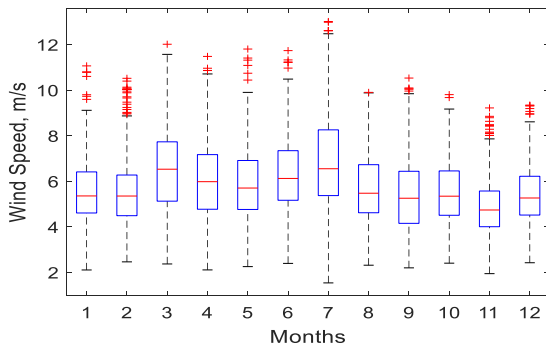
FIGURE 17. The wind speed at 10 m height for Arar site.

B. INPUT DATA PART

Many input data should be introduced to the computer program as shown in the following points:

- Hourly wind speed for a complete year,
  The hourly wind speed is shown in Figure 16 and the boxplot of the wind speed is shown in Figure 17. Also, the monthly and yearly average wind speed is shown in Table 1.

TABLE 1. Wind speed, solar irradiance on a horizontal surface, temperature for Arar city on 40 m height [67].

Month	Jan	Feb	Mar	April	May	June	July	Aug	Sep	Oct.	Nov	Dec	Mean
Wind speed	5.6	5.5	6.5	6.1	5.9	6.3	6.8	5.7	5.4	5.5	4.9	5.4	5.8
Solar Irradiance kWh/m²/d	5.58	6.15	7.07	7.29	7.61	7.48	7.78	7.55	7.39	6.66	5.64	4.85	6.75
Ta (ºC)	9.3	13.5	17.4	23.3	28.2	33.0	34.8	36	30.4	25.3	15.7	8.8	26.53

- Hourly solar irradiance and temperature for a complete year,
  The hourly solar irradiance is shown in Figure 18 and the boxplot of the solar irradiance is shown in Figure 19. Also, the monthly and yearly average solar irradiance is shown in Table 1.
- Hourly load demand for a complete year, (average load is 3.8078 MW)
  The hourly load along one year is collected from the isolated area in the north of Saudi Arabia is shown in Figure 20 and the boxplot of the hourly load curve is shown in Figure 21. The monthly weather data of Arar city are shown in Figure 22.
- Wind turbine specification parameters like the rated power P_R, cut-in, rated, and cut-out wind speed, hub-height, cost per kW, etc.,
  The specification parameters of the wind turbines are shown in Table 2.
- The PV module specification parameters, such as the module area, efficiency, price/m²,
  The specifications parameters of the PV modules used in the simulation are shown in Table 3.
- Battery specification parameters, such as the rated energy for each unit and the rated charging/discharging power, and the charging/discharging efficiencies, and the price of each battery,

TABLE 2. Wind Turbine parameters.

WT_cost	$1300/kW
OMC	$100/kW/year [68]
u_c	2.5m/s
u_r	8m/s
u_f	25m/s
P_R	60 kW per WT
Scale parameter c	5.5661
Shape parameter	2.5649
T_{WT}	20 year

TABLE 3. The PV specification parameters.

PV_COST	200/m²
PV_OMC	0.01*PV_cost [68]
PV_SL	25%
Area_module	1.67m2
efficiency	18%
T_{PV}	30 year
β_t	0.005 per °C
T_{cr}	25 °C

The specification parameters of the battery are shown in Table 4.

TABLE 4. The battery specification parameters.

Battery cost	$100/kWh [69]
BA_OMC	$0.02/kWh/year
BA_SL	20%*BA_cost
Battery life	5 years
η_{BC}	0.9
η_{BD}	0.95
σ	0.02%
DOD	70%

- Diesel generators specification parameters, such as the rated power, operating costs, and its price,
  The specifications of the Diesel generator parameters are shown in Table 5.
- AC/DC inverter cost and efficiency.
  The specification parameters are shown in Table 6.
- DC-DC converter and MPPT for the PV system rated values and price/kWh.
- The control parameters of the optimization technique (Such as ω, c_l, and c_g in the PSO). The control parameters of the PSO and BA are shown in Table 7 and Table 9, respectively.
- The tolerance for the stopping criterion.
- The general parameters like the paper lifetime, T, interest rate, and inflation rate are shown in Table 10.

VII. SIMULATION RESULTS

The optimization results of using the HES is done by using the PSO, BA, and SMO optimization tools. Three different studies are introduced in the simulation results part as shown in the following sections:

1. Evaluation of the best optimization technique.
2. The variation of the weight factor, M.
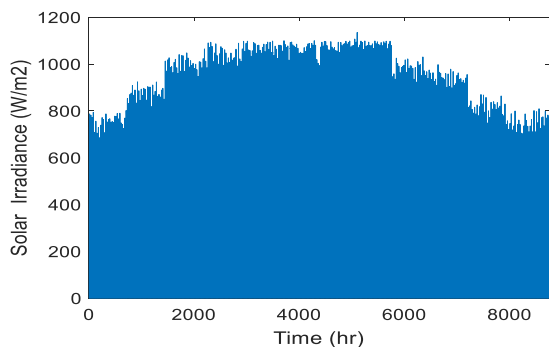3. The detailed results of the optimization technique in HES design.

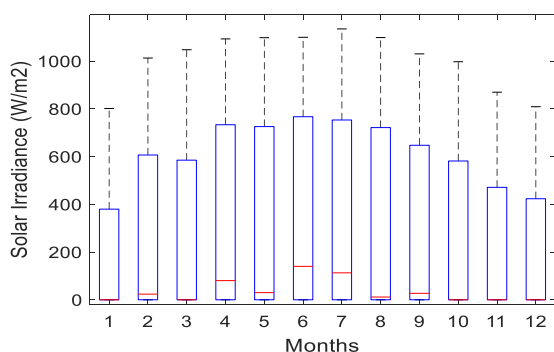**FIGURE 18.** Hourly solar irradiance on horizontal surface for Arar site.

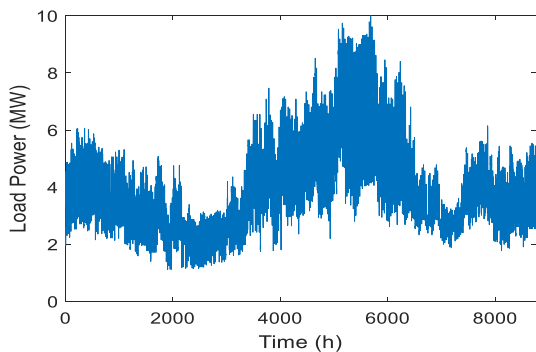**FIGURE 19.** The solar irradiance on horizontal surface for Arar site.
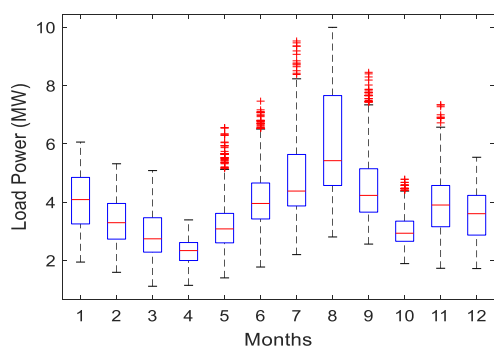

FIGURE 20. Hourly load power for Arar site.

FIGURE 21. Monthly load power for Arar site.

FIGURE 22. Monthly weather data of Arar city.

TABLE 5. The diesel generator specification parameters.

Parameter	Value
Cost/kW	$250/kW
Fuel cost	$0.9/L [55]
Lifetime (operating hours)	25000 hr
Minimum allowable load ratio	30%

TABLE 6. The inverter specifications parameters.

INV_cost	$325/kW
INV_OMC	$5/kW/year
INV_SL	$50/kW
T_{inv}	10 years
η_{inv}	0.95

TABLE 7. The PSO control parameters.

n	50
ω	0.9 to 0.4
c_l	1.49
c_g	1.49
It	100

TABLE 8. Bat algorithm control parameters.

f_{min}	0
f_{max}	2
ω	1
A_0	1
r_0	0.5
α, γ	0.95

TABLE 9. The general economic parameters.

Parameter	Value
l	4%
r	10%
T	20 years

A. EVALUATION OF THE BEST OPTIMIZATION TECHNIQUE

In this study, the detailed results of using the three different strategies PSO, BA, and SMO are evaluated to choose the best one of them. The eva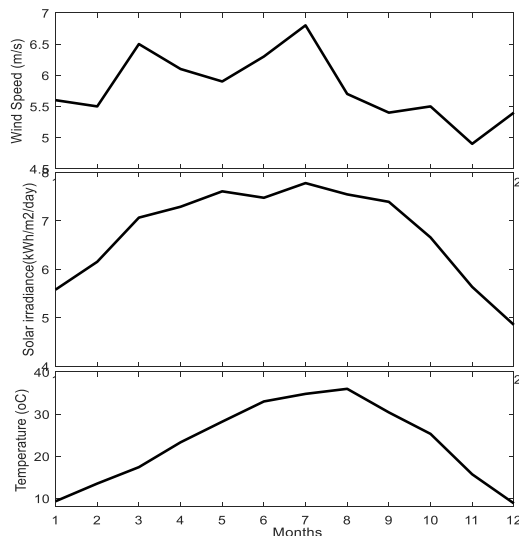luation criterion is based on the lowest failure rate and the fastest convergence time. In this analysis the weight value, *M* which is shown in (54) is selected to be; $M = 1$. For fair evaluation the swarm size for all optimization tools equal to 50 particles. Also, the parameters used in each technique are the same as introduced in the

TABLE 10. The variation of the number of WTs, PV area, size of the batteries, and the rated power of Diesel engine at $M = 1.0$.

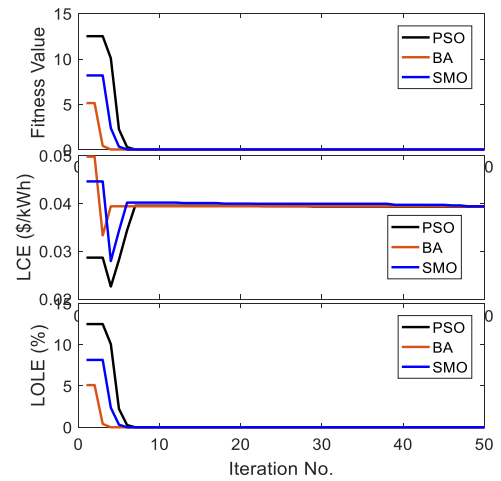| Item		Size	Energy Contribution	IC
Wind Energy	PED=-1	NWT=79, P_W=4740 kW	34.85 %	$6,162,000
	PED=0 (No DR)	NWT=91, P_W=5460 kW	33.97 %	$7,098,000
PV System	PED=-1	SCA=45128 m², P_{PVr}=8123 kW	63.36 %	$9,025,600
	PED=0 (No DR)	SCA=51781m², P_{PVr}=9320 kW	61.52 %	$10,356,200
Battery	PED=-1	E_{BR}=2715 kWh		$271,500
	PED=0 (No DR)	E_{BR}=5624 kWh		$562,400
Diesel	PED=-1	1000 kW	1.79 %	$300,000
	PED=0 (No DR)	2600 kW	4.51 %	$780,000
Inverter	PED=-1	8000 kW		$1,800,000
	PED=0 (No DR)	9500 kW		$2,137,500
Smart Grid cost	PED=-1			$1,200,000
	PED=0 (No DR)	0		0
IC	PED=-1			$18,759,100
	PED=0 (No DR)			$20,934,100
LCE	PED=-1			$0.0392/kWh
	PED=0 (No DR)			$0.0473/kWh

FIGURE 23. The convergence performance of the PSO, BA, SMO techniques.

FIGURE 24. The variation of the fitness function, LCE, and LOLE along with the weight value, M.

tables shown in the input data section where the $PED = -1$. The optimization performance of these optimization tools is performed for 10 different optimization runs as shown in Figure 23. It is clear from Figure 23 that the BA is the fastest convergence one where it captured the optimal solution after 5 iterations, the PSO captured the optimal solution after 8 iterations, meanwhile, the SMO captured the optimal solution after 45 iterations. Also, it is clear that all the optimization techniques captured the same global optimal solution where, the minimum fitness function is $0.0392 and the LOLE is zero, and the Levelized CoE (*LCE*) is $0.0392/kWh. From these results, it is clear that the BA is the fastest optimization technique where it captured the minimum solution with 5 iterations compared to 8, and 45 for PSO and SMO, respectively. Due to the superior results of the bat algorithm (BA) technique, it will be used in the following simulation studies.

B. THE VARIATION OF WEIGHT FACTOR, M

From the above study, the BA is having the best performance than the other two techniques and for this reason, it will be used in the next two simulation studies. The objective function used to reduce the cost and the *LOLE* is shown in (54). The weight value, *M* is multiplied by the *LCE* to give the required weight to the *LCE* compared to <u>*LOLE*</u>. The simulation in this study is performed for different values of *M* to see its response of the *LCW*, and *LOLE*. Figure 24 shows the variation of the fitness function, *LCW,* and *LOLE* along with the value of *M*. It is clear from Figure 24 that, with a low value of *M*, the cost is dropping very fast where it drops from $0.0.0393/kWh when *M* <1 to $0.02/kWh when *M* >1.2.

During the period $M < 1.2$ the *LOLE* is zero. During the period $1.2 < M < 4$ the LOLE is increased from zero to 0.3482. For the high value of M, the cost is saturated at $M > 1.2$ and the LOLE is still increasing and for this reason, it is better to use $M = 1.2$ to get the lowest cost at zero *LOLE* value.

C. THE DETAILED RESULTS OF THE OPTIMIZATION TECHNIQUE IN HES DESIGN

Based on the above simulation studies, the best metaheuristic technique was the BA and the best weight value, *M* is 1.0, which will be used in this study. The variation of the number of WTs, PV area, size of the batteries, and the rated power of Diesel engine at $M = 1.0$ when using DR with PED $= -1$ and without DR at LOLE $= 0.0$ are shown in Table 10. It is clear from this table that the sizes of all components are reduced when using the smart grid concept with DR ($PED = -1$) compared to the values without using DR into consideration ($PED = 0.0$). Also, the total initial cost of the HES when using the smart grid concept is $18,759,100

compared to $20,934,100 when the DR did not use. Also, the use of DR reduced the Levelized CoE from $0.0473/kWh to $0.0392/kWh when used the smart grid concept ($PED = -1$) compared to the condition that does not consider the smart grid concept. The reduction in *LCE* is 20.66% when using the smart grid concept into consideration compared to the traditional design of the HES which does not consider the DR.

VIII. CONCLUSION

RES are becoming promised option in the modern power system energy mix. Wind and PV energies are the most frequently used RES. The output power from these sources is having intermittent nature which makes them cannot work alone to supply a load with its need for energy in acceptable reliability. For this reason, these sources should be connected to the utility grid or should be connected with battery storage and Diesel energy system in case of off-grid applications especially in rural areas. In the case of off-grid hybrid energy systems (HES), the size of the components should be chosen to feed the load with all normal and abnormal operating conditions which make the sizes of components are very large. The sizing of the HES is introduced in literature without using the SGC which make the HES is not cost-effective and reduces its reliability. A novel demand response (DR) strategy is introduced in this article to model the response of the customers to the dynamic change of the tariff. This novel DR strategy has been used in the sizing of the HES to reduce the size of HES and reduces the CoE generated compared to the traditional sizing of the HES without using the DR into consideration. The use of the new DR strategy has achieved zero loss of energy expected at a very low price. The design of the HES using a smart grid has been optimized using three modern swarm optimization control namely, particle swarm optimization (PSO), bat algorithm (BA), and Social mimic optimization (SMO). The detailed analysis for the results obtained from these optimization techniques showed that the BA is the fastest and most reliable technique where it captured the minimum cost and optimal size of components with 5 iterations, meanwhile, the PSO and the SMO need 8 and 45 iterations, respectively. The initial cost of the HES is $18,759,100 when using a smart grid and DR strategy into consideration, compared to $20,934,100 for the traditional sizing of the HES without a smart grid. Moreover, the Levelized CoE is $0.0392/kWh when using a smart grid and DR in the design stage compared to $0.473/kWh when the traditional design of HES is used. This cost reduction is 20.66% compared to the cost calculated based on the traditional sizing technique which proves the superiority of using the DR into consideration when sizing the HES.

REFERENCES

[1] S. Sinha and S. S. Chandel, "Review of recent trends in optimization techniques for solar photovoltaic–wind based hybrid energy systems," *Renew. Sustain. Energy Rev.*, vol. 50, pp. 755–769, Oct. 2015.

[2] A. M. Eltamaly and A. A. Al-Shamma'a, "Optimal configuration for isolated hybrid renewable energy systems," *J. Renew. Sustain. Energy*, vol. 8, no. 4, Jul. 2016, Art. no. 045502.

[3] L. K. Gan, J. K. H. Shek, and M. A. Mueller, "Hybrid wind–photovoltaic–diesel–battery system sizing tool development using empirical approach, life-cycle cost and performance analysis: A case study in Scotland," *Energy Convers. Manage.*, vol. 106, pp. 479–494, Dec. 2015.

[4] A. Tiwary, S. Spasova, and I. D. Williams, "A community-scale hybrid energy system integrating biomass for localised solid waste and renewable energy solution: Evaluations in U.K. and Bulgaria," *Renew. Energy*, vol. 139, pp. 960–967, Aug. 2019.

[5] S. Upadhyay and M. P. Sharma, "Development of hybrid energy system with cycle charging strategy using particle swarm optimization for a remote area in India," *Renew. Energy*, vol. 77, pp. 586–598, May 2015.

[6] A. J. Litchy and M. H. Nehrir, "Real-time energy management of an islanded microgrid using multi-objective Particle Swarm Optimization," in *Proc. PES Gen. Meeting | Conf. Expo. IEEE*, 2014, pp. 1–5.

[7] D. Parra, M. Swierczynski, D I. Stroe, S. A. Norman, A. Abdond, J. Worlitschek, T. O'Dohertye, L. Rodrigues, M. Gillott, X. Zhang, C. Bauer, and M. K. Patela, "An interdisciplinary review of energy storage for communities: Challenges and perspectives," *Renew. Sustain. Energy Rev.*, vol. 79, pp. 730–749, Nov. 2017.

[8] M. S. Guney and Y. Tepe, "Classification and assessment of energy storage systems," *Renew. Sustain. Energy Rev.*, vol. 75, pp. 1187–1197, Aug. 2017.

[9] M. A. Mohamed, A. M. Eltamaly, A. I. Alolah, and A. Y. Hatata, "A novel framework-based cuckoo search algorithm for sizing and optimization of grid-independent hybrid renewable energy systems," *Int. J. Green Energy*, vol. 16, no. 1, pp. 86–100, Jan. 2019.

[10] M. L. Kolhe, K. M. I. U. Ranaweera, and A. G. B. S. Gunawardana, "Techno-economic sizing of off-grid hybrid renewable energy system for rural electrification in Sri Lanka," *Sustain. Energy Technol. Assessments*, vol. 11, pp. 53–64, Sep. 2015.

[11] W. Zhou, C. Lou, Z. Li, L. Lu, and H. Yang, "Current status of research on optimum sizing of stand-alone hybrid solar–wind power generation systems," *Appl. Energy*, vol. 87, no. 2, pp. 380–389, Feb. 2010.

[12] A. T. D. Perera, R. A. Attalage, K. K. C. K. Perera, and V. P. C. Dassanayake, "Designing standalone hybrid energy systems minimizing initial investment, life cycle cost and pollutant emission," *Energy*, vol. 54, pp. 220–230, Jun. 2013.

[13] R. Wang, G. Li, M. Ming, G. Wu, and L. Wang, "An efficient multi-objective model and algorithm for sizing a stand-alone hybrid renewable energy system," *Energy*, vol. 141, pp. 2288–2299, Dec. 2017.

[14] U. Bawah, K. E. Addoweesh, and A. M. Eltamaly, "Comparative study of economic viability of rural electrification using renewable energy resources versus diesel generator option in Saudi Arabia," *J. Renew. Sustain. Energy*, vol. 5, no. 4, Jul. 2013, Art. no. 042701.

[15] M. A. Mohamed, A. M. Eltamaly, and A. I. Alolah, "Swarm intelligence-based optimization of grid-dependent hybrid renewable energy systems," *Renew. Sustain. Energy Rev.*, vol. 77, pp. 515–524, Sep. 2017.

[16] F. A. Khan, N. Pal, and S. H. Saeed, "Review of solar photovoltaic and wind hybrid energy systems for sizing strategies optimization techniques and cost analysis methodologies," *Renew. Sustain. Energy Rev.*, vol. 92, pp. 937–947, Sep. 2018.

[17] A. M. Eltamaly and M. A. Mohamed, "Optimal sizing and designing of hybrid renewable energy systems in smart grid applications," in *Advances in Renewable Energies and Power Technologies*. Amsterdam, The Netherlands: Elsevier, 2018, pp. 231–313.

[18] M. A. Mohamed, A. M. Eltamaly, and A. I. Alolah, "Sizing and techno-economic analysis of stand-alone hybrid photovoltaic/wind/diesel/battery energy systems," *J. Renew. Sustain. Energy*, vol. 7, no. 6, 2015, Art. no. 063128.

[19] M. A. Mohamed, A. M. Eltamaly, and A. I. Alolah, "PSO-based smart grid application for sizing and optimization of hybrid renewable energy systems," *PLoS ONE*, vol. 11, no. 8, Aug. 2016, Art. no. e0159702.

[20] B. S. Borowy and Z. M. Salameh, "Methodology for optimally sizing the combination of a battery bank and PV array in a wind/PV hybrid system," *IEEE Trans. Energy Convers.*, vol. 11, no. 2, pp. 367–375, Jun. 1996.

[21] T. Markvart, "Sizing of hybrid PV-wind energy systems," *Sol. Energy*, vol. 59, no. 4, pp. 277–281, 1996.

[22] S. Ashok, "Optimised model for community-based hybrid energy system," *Renew. Energy*, vol. 32, no. 7, pp. 1155–1164, Jun. 2007.

[23] H. H. El-Tamaly, M. Hamada, and A. M. Eltamaly, "Computer simulation of wind energy system and applications," in *Proc. Int. AMSE Conf. Syst. Anal., Control Designs (AMSE)*, vol. 4, 1995, pp. 84–94.

[24] A. M. Eltamaly, K. E. Addoweesh, U. Bawah, and M. A. Mohamed, "New software for hybrid renewable energy assessment for ten locations in Saudi Arabia," *J. Renew. Sustain. Energy*, vol. 5, no. 3, May 2013, Art. no. 033126.

[25] A. D. Bagul, Z. M. Salameh, and B. Borowy, "Sizing of a stand-alone hybrid wind-photovoltaic system using a three-event probability density approximation," *Sol. Energy*, vol. 56, no. 4, pp. 323–335, Apr. 1996.

[26] G. Tina, S. Gagliano, and S. Raiti, "Hybrid solar/wind power system probabilistic modelling for long-term performance assessment," *Sol. Energy*, vol. 80, no. 5, pp. 578–588, May 2006.

[27] R. Chedid, H. Akiki, and S. Rahman, "A decision support technique for the design of hybrid solar-wind power systems," *IEEE Trans. Energy Convers.*, vol. 13, no. 1, pp. 76–83, Mar. 1998.

[28] A. Kaabeche, S. Diaf, and R. Ibtiouen, "Firefly-inspired algorithm for optimal sizing of renewable hybrid system considering reliability criteria," *Sol. Energy*, vol. 155, pp. 727–738, Oct. 2017.

[29] R. V. Barenji, M. G. Nejad, and I. Asghari, "Optimally sized design of a wind/photovoltaic/fuel cell off-grid hybrid energy system by modified-gray wolf optimization algorithm," *Energy Environ.*, vol. 29, no. 6, pp. 1053–1070, Sep. 2018.

[30] A. Maleki, M. A. Nazari, and F. Pourfayaz, "Harmony search optimization for optimum sizing of hybrid solar schemes based on battery storage unit," *Energy Rep.*, vol. 6, pp. 102–111, Dec. 2020.

[31] W. Zhang, A. Maleki, M. A. Rosen, and J. Liu, "Optimization with a simulated annealing algorithm of a hybrid system for renewable energy including battery and hydrogen storage," *Energy*, vol. 163, pp. 191–207, Nov. 2018.

[32] S. Singh and S. C. Kaushik, "Optimal sizing of grid integrated hybrid PV-biomass energy system using artificial bee colony algorithm," *IET Renew. Power Gener.*, vol. 10, no. 5, pp. 642–650, May 2016.

[33] A. K. Pandey and S. Kirmani, "Multi-objective optimal location and sizing of hybrid photovoltaic system in distribution systems using crow search algorithm," *Int. J. Renew. Energy Res.*, vol. 9, no. 4, pp. 1681–1693, 2019.

[34] S. Balochian and H. Baloochian, "Social mimic optimization algorithm and engineering applications," *Expert Syst. Appl.*, vol. 134, pp. 178–191, Nov. 2019.

[35] A. Roscoe and G. Ault, "Supporting high penetrations of renewable generation via implementation of real-time electricity pricing and demand response," *IET Renew. Power Genera.*, vol. 4, no. 4, pp. 369–382, 2010, doi: 10.1049/iet-rpg.2009.0212.

[36] M. L. Crow, B. Mcmillin, W. Wang, and S. Bhattacharyya, "Intelligent energy management of the FREEDM system," in *Proc. IEEE PES Gen. Meeting*, Providence, RI, USA, Jul. 2010, pp. 1–4, doi: 10.1109/PES.2010.5589992.

[37] F. Rahimi and A. Ipakchi, "Overview of demand response under the smart grid and market paradigms," in *Proc. Innov. Smart Grid Technol. (ISGT)*, Gothenburg, Sweden, Jan. 2010, pp. 1–7, doi: 10.1109/ISGT.2010.5434754.

[38] C. Cecati, C. Citro, A. Piccolo, and P. Siano, "Smart operation of wind turbines and diesel generators according to economic criteria," *IEEE Trans. Ind. Electron.*, vol. 58, no. 10, pp. 4514–4525, Oct. 2011, doi: 10.1109/TIE.2011.2106100.

[39] R. Deng, Z. Yang, M.-Y. Chow, and J. Chen, "A survey on demand response in smart grids: Mathematical models and approaches," *IEEE Trans. Ind. Informat.*, vol. 11, no. 3, pp. 570–582, Jun. 2015.

[40] H. A. Aalami, M. P. Moghaddam, and G. R. Yousefi, "Demand response modeling considering interruptible/curtailable loads and capacity market programs," *Appl. Energy*, vol. 87, no. 1, pp. 243–250, Jan. 2010.

[41] J. Saebi, H. Taheri, J. Mohammadi, and S. S. Nayer, "Demand bidding/buyback modeling and its impact on market clearing price," in *Proc. IEEE Int. Energy Conf.*, Dec. 2010, pp. 791–796.

[42] R. Tyagi and J. W. Blac, "Emergency demand response for distribution system contingencies," in *Proc. IEEE PES Transmiss. Distrib. Conf. Expo.*, Apr. 2010, pp. 1–4.

[43] K. Herter, "Residential implementation of critical-peak pricing of electricity," *Energy Policy*, vol. 35, no. 4, pp. 2121–2130, Apr. 2007.

[44] S. Borenstein, "Equity effects of increasing-block electricity pricing," Center Study Energy Markets, Univ. California Energy Inst., Berkeley, CA, USA, Tech. Rep. CSEM WP 180, 2008.

[45] P. Samadi, A.-H. Mohsenian-Rad, R. Schober, V. W. S. Wong, and J. Jatskevich, "Optimal real-time pricing algorithm based on utility maximization for smart grid," in *Proc. 1st IEEE Int. Conf. Smart Grid Commun.*, Oct. 2010, pp. 415–420.

[46] P. Samadi, H. Mohsenian-Rad, R. Schober, and V. W. S. Wong, "Advanced demand side management for the future smart grid using mechanism design," *IEEE Trans. Smart Grid*, vol. 3, no. 3, pp. 1170–1180, Sep. 2012.

[47] A.-H. Mohsenian-Rad, V. W. S. Wong, J. Jatskevich, and R. Schober, "Optimal and autonomous incentive-based energy consumption scheduling algorithm for smart grid," in *Proc. Innov. Smart Grid Technol. (ISGT)*, Jan. 2010, pp. 1–6.

[48] A.-H. Mohsenian-Rad, V. W. S. Wong, J. Jatskevich, R. Schober, and A. Leon-Garcia, "Autonomous demand-side management based on game-theoretic energy consumption scheduling for the future smart grid," *IEEE Trans. Smart Grid*, vol. 1, no. 3, pp. 320–331, Dec. 2010.

[49] S. Wang, X. Xue, and C. Yan, "Building power demand response methods toward smart grid," *HVAC R Res.*, vol. 20, no. 6, pp. 665–687, Aug. 2014.

[50] V. Zambrana and M. Norman, "System design and analysis of a renewable energy source powered microgrid," Ph.D. dissertation, Dept. Syst. Eng., Univ. Maryland, College Park, MD, USA, 2018.

[51] E. Skoplaki, A. G. Boudouvis, and J. A. Palyvos, "A simple correlation for the operating temperature of photovoltaic modules of arbitrary mounting," *Sol. Energy Mater. Sol. Cells*, vol. 92, no. 11, pp. 1393–1402, Nov. 2008.

[52] A. Kaabeche, M. Belhamel, and R. Ibtiouen, "Optimal sizing method for stand-alone hybrid PV/wind power generation system," in *Proc. SMEE*, 2010, pp. 205–213.

[53] H. Yang, W. Zhou, L. Lu, and Z. Fang, "Optimal sizing method for stand-alone hybrid solar–wind system with LPSP technology by using genetic algorithm," *Sol. Energy*, vol. 82, no. 4, pp. 354–367, Apr. 2008.

[54] Y. A. Katsigiannis, P. S. Georgilakis, and E. S. Karapidakis, "Hybrid simulated annealing–tabu search method for optimal sizing of autonomous power systems with renewables," *IEEE Trans. Sustain. Energy*, vol. 3, no. 3, pp. 330–338, Jul. 2012.

[55] (2020). *Diesel Generator Price*. [Online]. Available: https://www.globalpetrolprices.com/

[56] V. O. Okinda and N. O. Abungu, "A review of techniques in optimal sizing of hybrid renewable energy systems," *Int. J. Res. Eng. Technol.*, vol. 4, no. 11, pp. 153–163, 2015.

[57] S. Sanajaoba and E. Fernandez, "Maiden application of cuckoo search algorithm for optimal sizing of a remote hybrid renewable energy system," *Renew. Energy*, vol. 96, pp. 1–10, Oct. 2016.

[58] F. Mostofi and H. Shayeghi, "Feasibility and optimal reliable design of renewable hybrid energy system for rural electrification in Iran," *Int. J. Renew. Energy Res.*, vol. 2, no. 4, pp. 574–582, 2012.

[59] A. A. Lazou and A. D. Papatsoris, "The economics of photovoltaic stand-alone residential households: A case study for various European and mediterranean locations," *Sol. Energy Mater. Sol. Cells*, vol. 62, no. 4, pp. 411–427, Jun. 2000.

[60] S. Diaf, M. Belhamel, M. Haddadi, and A. Louche, "Technical and economic assessment of hybrid photovoltaic/wind system with battery storage in Corsica island," *Energy Policy*, vol. 36, no. 2, pp. 743–754, Feb. 2008.

[61] R. Bazyar, K. Valipoor, M. R. Javadi, M. Valizade, and H. Kord, "Optimal design and energy management of stand-alone wind/PV/diesel/battery using bacterial foraging algorithm," in *Proc. 8th Int. Energy Conf.*, 2011, pp. 1–14.

[62] X.-S. Yang, "A new metaheuristic bat-inspired algorithm," in *Nature Inspired Cooperative Strategies for Optimization (NICSO 2010)*. Berlin, Germany: Springer, 2010, pp. 65–74.

[63] J. Kennedy and R. Eberhart, "Particle swarm optimization," in *Proc. Int. Conf. Neural Netw.*, vol. 4, Nov./Dec. 1995, pp. 1942–1948.

[64] M. Jakubcová, P. Máca, and P. Pech, "A comparison of selected modifications of the particle swarm optimization algorithm," *J. Appl. Math.*, vol. 2014, Jun. 2014, Art. no. 293087.

[65] A. Eltamaly, H. M. H. Farh, and M. S. Al Saud, "Impact of PSO reinitialization on the accuracy of dynamic global maximum power detection of variant partially shaded PV systems," *Sustainability*, vol. 11, no. 7, p. 2091, Apr. 2019.

[66] A. M. Eltamaly, M. S. Al-Saud, and A. G. Abokhalil, "A novel bat algorithm strategy for maximum power point tracker of photovoltaic energy systems under dynamic partial shading," *IEEE Access*, vol. 8, pp. 10048–10060, 2020.

[67] M. A. M. Ramli, S. Twaha, and Z. Al-Hamouz, "Analyzing the potential and progress of distributed generation applications in Saudi Arabia: The case of solar and wind resources," *Renew. Sustain. Energy Rev.*, vol. 70, pp. 287–297, Apr. 2017.

[68] A. Maleki, F. Pourfayaz, and M. A. Rosen, "A novel framework for optimal design of hybrid renewable energy-based autonomous energy systems: A case study for Namin, Iran," *Energy*, vol. 98, pp. 168–180, Mar. 2016.

[69] R. N. S. R. Mukhtaruddin, H. A. Rahman, M. Y. Hassan, and J. J. Jamian, "Optimal hybrid renewable energy design in autonomous system using iterative-Pareto-fuzzy technique," *Int. J. Electr. Power Energy Syst.*, vol. 64, pp. 242–249, Jan. 2015.

• • •